Diagnosis from MRI Images: A deep learning approach

Mohamed Rifat A K
Associate Software Engineer
Bosch Global Software Technologies Pvt. Ltd
Bengaluru, India

Sabitha S
Graduate Engineer Trainee
HCL Technologies Pvt. Ltd
Chennai, India

***Abstract*— Brain tumors are either cancerous or non-cancerous masses of abnormal brain cells. In this paper, we look at three different types of brain tumors: Meningioma tumor, glioma tumor, and pituitary tumor. Brain tumor segmentation is a critical diagnostic method for brain tumor detection and diagnosis. Brain tumor segmentation from MRI can be done manually, but the accuracy and identification are poor. The classification of abnormalities is a time-consuming task for physicians because it is not predictable and straightforward. However, tumor detection is difficult because tumors have complex appearances and boundary characteristics. A report depicts the doctor's diagnosis of a brain tumor. This paperwork describes an automated detection and diagnosis of brain tumors using MRI images via EfficientNet, where we built a system that automatically generates a preliminary report that includes the type of tumor, its corresponding ICD code, tumor diameter and area, as well as the original input image with the tumor highlighted for visualization. This will be accomplished through the classification and segmentation of MRI images, with classification using Dense EfficinetNet to identify the tumor type and ICD code and segmentation using EfficientNet UNet to visualize the tumor and determine its diameter and area. A preliminary report for our paper is being created, which will use one MRI image of a brain tumor to diagnose tumor diameter and tumor area.**

Keywords—Brain Tumor, Detection, Diagnosis, EfficientNet, Classification, Segmentation

I. INTRODUCTION

A. Brain Tumor

A brain tumor is an abnormal growth of brain cells that can be malignant or non-cancerous. A brain tumor can cause new or worsening headaches, impaired vision, loss of balance, disorientation, and seizures. There may be no symptoms in certain cases. Tumors in the brain can form, or cancer from other parts of the body can spread to the brain. Treatment options include surgery, radiation, and chemotherapy [1]. Brain tumors account for 85-90% of all primary central nervous system (CNS) tumors. An estimated 308,102 people worldwide will be diagnosed with a primary brain or spinal cord tumors in 2020. In the United States this year, approximately 4,170 children under the age of 15 will be diagnosed with brain or CNS tumors. [2]. The three more common types of brain tumor which we have detected and diagnosed in our paper is shown below:

1) Meningioma: Meningioma is a tumor that develops in the membranes that surround the brain and spinal cord, known as the meninges. It is classified as a brain tumor even though it is not strictly a brain tumor because it has the potential to compress or press on nearby brains, nerves, and arteries. The most frequent type of tumor that arises in the head is meningioma. The vast majority of meningiomas grow slowly and often go unnoticed for years. On the other hand, their impact on neighboring brain tissue, nerves, or arteries can sometimes result in significant disability. Meningiomas are more frequent in women and are diagnosed later in life, but they can strike at any age [3]. Most meningiomas do not require immediate treatment since they grow slowly and frequently without generating any symptoms.

2) Glioma: Glioma is a form of brain tumor that can damage the brain as well as the spinal cord. Gliomas start in the gluey supporting cells (glial cells) that surround nerve cells and help them operate. Glial cells can become tumors in three ways. Gliomas are categorized based on the type of glial cell involved in the tumor and the tumor's genetic traits, which can help predict how the tumor will behave over time and which treatments will be most effective. A glioma can impede brain function and be fatal depending on its location and rate of growth. Gliomas are an extremely prevalent kind of primary brain tumor [4]. The type of glioma a patient has an impact on therapy and prognosis. Glioma treatment options include surgery, radiation therapy, chemotherapy, targeted therapy, and experimental clinical trials [4].

3) Pitituary Tumor: Pituitary tumors are malignant growths in the pituitary gland that develops over time. Some pituitary tumors overproduce hormones that control important physiological functions. The pituitary gland may produce fewer hormones as a result of some pituitary tumors. Pituitary tumors are almost always benign (noncancerous) growths (adenomas). Adenomas are benign tumors that do not spread outside of the pituitary gland or surrounding organs. Surgical removal, growth control, and hormone-level pharmaceutical therapy are among the options for treating pituitary tumors. Observation is possible [5]. Figure 1 shows the MRI image of the three different brain tumors.

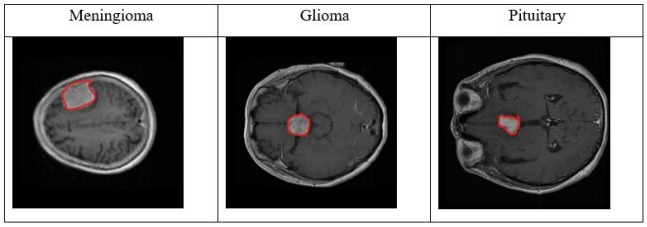

Fig. 1. MRI image of the brain tumors.

B. Brain Tumor Diagnosis

To locate and diagnose a brain tumor, as well as to determine the type of tumor, doctors use imaging studies to determine if the tumor is a primary brain tumor or cancer that has spread to the brain from elsewhere in the body. Images of the inside of the body are produced via imaging tests [6]. When choosing a diagnostic test, doctors may consider the type of tumor suspected, signs and symptoms, age and general health, the findings of previous medical tests, and so on. In general, magnetic resonance imaging is used to diagnose a brain tumor (MRI). A preliminary report is being created for our paper that uses one MRI scan of a brain tumor to determine tumor diameter and tumor area. The following factors are considered in the preliminary report.

1) Tumor type: For our paper, we are going to focus on detection and diagnosis of the three types of brain tumor: meningioma, glioma and pituitary.

2) ICD Code: The International Classification of Diseases (ICD) is a system for collecting, processing, classifying, and presenting mortality information that promotes international comparability [7]. For meningioma tumor, the corresponding ICD code is D32.9, For glioma tumor, the corresponding ICD code is C71.9, and for pituitary tumor, the corresponding ICD code is E23.7.

3) Tumor Diameter: On pathologic evaluation, tumor diameter is defined as the maximum size of the invasive component of the primary tumor [8].

4) Tumor Area: The tumor area is defined as (tumor length) × (maximum tumor depth) [8].

C. EfficientNet for Brain Tumor Diagnosis

Brain tumor segmentation is an important method of diagnosis for improving brain tumor patients' survival rates and developing a better treatment procedure in medical image processing. Manual brain tumor segmentation using an MRI for detection and diagnosis is possible, but it has a low level of accuracy and identification. The classification of abnormalities is not only unpredictable and difficult for doctors, but it is also time-consuming. Nowadays, automatic segmentation and analysis of brain tumors is a hot research topic. Tumor detection, on the other hand, is a difficult task due to the complexity of tumor appearance and boundary features [9].

EfficientNet is a more practical choice for real-world applications where resource constraints are a major concern such as brain tumor detection and diagnosis. Furthermore, EfficientNet has been shown to outperform other popular pre-trained models such as ResNet, Inception, and VGG on a variety of image classification benchmarks in transfer learning which makes it an ideal choice for classification and segmentation of brain tumor detection and diagnosis.

D. Objectives

This paper presents an Efficient Net based detection and diagnosis of brain tumors using MRI images, where we build a system that automatically generates a preliminary report which contains the type of tumor, its corresponding ICD code, tumor diameter and tumor area along with the original input image with the tumor highlighted for visualization. This will be achieved through the classification and segmentation of MRI images with efficientnet as the base pretrained model, where the classification is done to identify the tumor type and ICD code and segmentation is done to visualize the tumor and to find its size and area. For our paper, a preliminary report is being constructed which utilizes one MRI image of a brain tumor to diagnose tumor diameter and tumor area.

II. Literature Survey

This chapter presents the literature survey on EfficientNet-Based Brain Tumor Detection and Diagnosis from MRI Images

Meiyan Huang et al., (2014) [10] created a content-based image retrieval (CBIR) system for retrieving T1-weighted contrast-enhanced magnetic resonance imaging (CE-MR) pictures of brain malignancies. The system uses the bag-of-visual-words (BoVW) model with partition learning to extract informative features for representing image contents. In addition, the Rank Error-based Metric Learning (REML) distance metric learning algorithm is presented to bridge the semantic gap between low-level visual data and high-level semantic concepts. The suggested method is tested on a brain T1-weighted CE-MR dataset with three different types of brain cancers (i.e., meningioma, glioma, and pituitary tumor).When compared to the spatial pyramid BoVW approach, the mean average precision (mAP) of retrieval increases beyond 4.6 percent when using the BoVW model with partition learning. In terms of mAP, the distance metric taught by REML surpasses three other known distance metric learning methods. Their proposed strategy increases the mAP of the CBIR system to 91.8 percent, and the precision to 93.1 percent when the system returns the top 10 images. These first findings show that the proposed strategy for retrieving brain tumors in T1-weighted CE-MR images is effective and practicable. Using the proposed method, the precision of the system can achieve 91.8 percent, and when the top 10 images are returned, the precision can reach 93.1 percent.

Jun Cheng et al., (2015) [11] their study focuses on the classification of three types of brain tumors in T1-weighted contrast-enhanced MRI (CE-MRI) images (meningioma, glioma, and pituitary tumor). For natural scene classification, spatial pyramid matching (SPM), which divides the image into increasingly fine rectangular subregions and computes histograms of local features from each subregion, produces excellent results. Because of the wide range of tumor shape and size, this method is not relevant to brain tumors. The authors offer an approach to improve classification performance in this paper. Using enhanced tumor region as ROI improves accuracies from 71.39 percent to 82.31 percent, 84.75 percent to 78.18 percent, and 88.19 percent to 83.54 percent for intensity histogram, GLCM, and BoW model, respectively, when compared to using tumor region as ROI. Ring-form partition had improved accuracies by up to 87.54 percent, 89.72 percent, and 91.28 percent, in addition to region augmentation.

Hossom H.Sultan et al., (2019) [12] using two publicly accessible datasets, they proposed a DL model based on a convolutional neural network to categorize different brain tumor kinds. The first divides tumors into categories (meningioma, glioma, and pituitary tumor). The other

differentiates between the three forms of glioblastoma (Grade A, B, and C).The first and second datasets, respectively, contain 233 and 73 patients with a total of 3064 and 516 photos on T1 weighted contrast-enhanced images. Starting with the input layer, which retains the pre-processed images and continuing through the convolution layers and their activation functions, the proposed network is made up of sixteen layers (3 convolution, 3 ReLU, normalization and 3 Max Pooling layers). Two dropout layers are also employed to avoid overfitting, followed by a fully connected layer and a SoftMax layer to predict the output, and finally a classification layer to yield the predicted class. Even though the dataset is small (due to the variety of imaging viewpoints), data augmentation assisted in producing better results and thus overcoming this issue. In the dataset considered in this work, their proposed architecture attained accuracy of 96.13 percent.

Ali Mohammad Alqudah et al., (2019) [13] utilized Convolutional Neural Network (CNN), one of the most extensively used deep learning architectures to classify a dataset of 3064 T1 weighted contrast-enhanced brain MR images into three groups for grading (classifying) brain cancers (Glioma, Meningioma, and Pituitary Tumor). The primary goal and purpose for this study are to develop a new CNN architecture for grading (classifying) brain cancers using T1-weighted contrast-enhanced brain MR images. The cropped and uncropped brain tumor photographs are saved in a database, and three folders are formed, one for each kind of glioma, meningioma, and pituitary tumor. In this paper, a new CNN architecture is used. The design has eighteen layers to allow the classifier to accurately grade the brain tumor. The dataset was separated into three subsets: training, validation, and testing, with percentages of 70%, 15%, and 15%, respectively. The suggested approach efficiently evaluated the brain tumor, with accuracy rates of 97.4 percent, 99.0 percent, and 99.2 percent for cropped lesions and 97.5 percent, 97.6 percent, and 98.4 percent for uncropped lesions. Most of the approaches presented in the literature in this study have obtained high recognition rates, with the highest being 97 percent. The design was successful in classifying brain tumors into three classifications with good accuracy and sensitivity in all dataset cases: uncropped, cropped, and segmented.

Dillip Ranjan Nayak et al., (2022) [14] their study suggests using min-max normalization to categorize 3260 T1-weighted contrast enhanced brain magnetic resonance images into four categories using a CNN-based dense EfficientNet (glioma, meningioma, pituitary, and no tumor). The constructed network is a dense EfficientNet that includes dense and drop-out layers. Boost the contrast of tumor cells, the authors coupled data augmentation with min-max normalization. The dense CNN model has the advantage of being able to accurately categorize a small database of images. As a result, the proposed method achieves outstanding overall results. The suggested model was 99.97% correct during training and 97.78% accurate during testing, according to the experimental results. The newly created EfficientNet CNN architecture can be a beneficial decision-making tool in the research of brain tumor diagnostic tests, thanks to its excellent accuracy and favourable F1 score.

III. Proposed Methodology

Figure 2 shows the overall proposed methodology for preliminary report generation.

A. Dataset

Jun Cheng et al., (2015) [15] proposed a brain tumor dataset. It is an open-source dataset obtained from Nanfang Hospital in Guangzhou and General Hospital at Tianjin Medical University in China between 2005 and 2010. The dataset was first made available online in 2015, and the most recent version was released in 2017. The Ethics Committees of Nanfang Hospital and General Hospital Tianjin Medical University in China have approved this dataset. Jun Cheng, School of Biomedical Engineering, Southern Medical University, Guangzhou, China, provided this dataset. The dataset contains 3064 T1-weighted contrast enhanced MRI slices. The images were taken in three planes: transverse, sagittal, and coronal. The dataset shows three types of brain tumors: meningioma, glioma, and pituitary tumors. Each slice has 512 x 512 pixels with a pixel size of 0.49mm x 0.49mm. Three experienced radiologists consulted the patient pathology report to determine the pathology type and then labelled the images for each patient. Each radiologist handled each image independently. In this dataset, each patient is represented solely by their Patient ID.

The Dataset contains Meningioma (708 slices), Glioma (1426 slices), and Pituitary tumor (930 slices). This data is organized in MATLAB data format (.mat file). Each file stores a struct containing the following fields for an image:

- cjdata.label: 1 for meningioma, 2 for glioma, 3 for pituitary tumor
- cjdata.PID: patient ID cjdata.image: image data
- cjdata.tumorBorder: A vector storing the coordinates of discrete points on tumor border. For example, [x1, y1, x2, y2,...] in which x1, y1 are planar coordinates on tumor border. It was generated by manually delineating the tumor border. So, we can use it to generate binary image of tumor mask.
- cjdata.tumorMask: A binary image with 1s indicating tumor region.

For Building a system which automatically generates a preliminary report for detection and diagnosis of brain tumor using a given MRI image, we are adding a healthy control dataset obtained from Kaggle [16]. There are 501 healthy images which are together added with the dataset bringing the total count of MRI images from 3064 images to 3565 images.

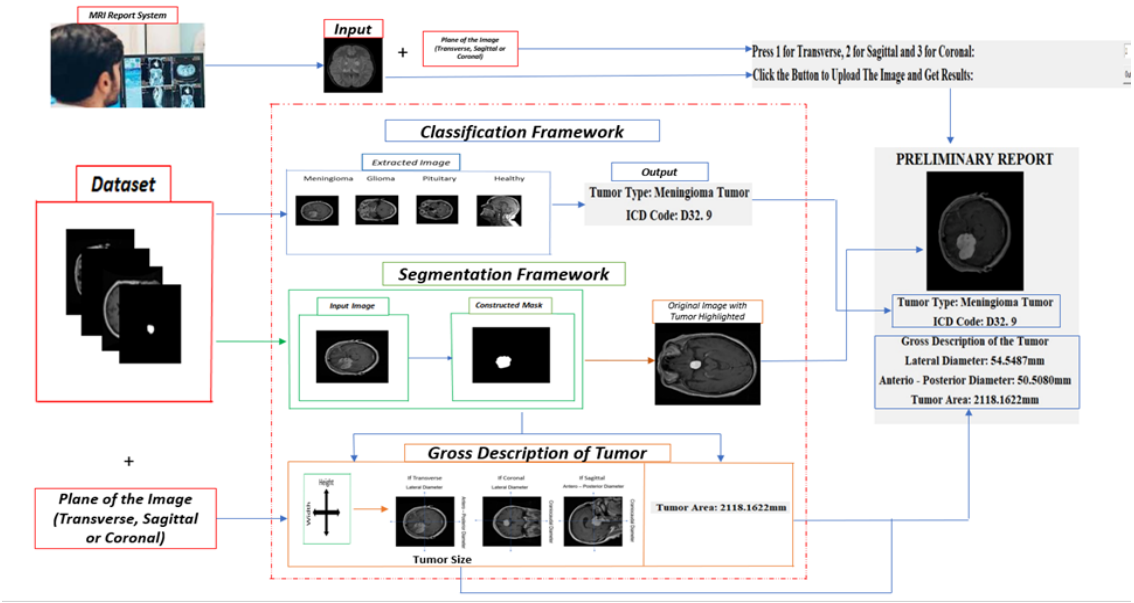

Fig. 2. Overall proposed methodology for preliminary report generation

Table 1 shows the number of images present across each classes of tumor along with their planes and the corresponding images present along them.

TABLE I. NO. OF IMAGES PRESENT IN EACH CATEGORY AND VIEWS

Tumor Category	No. of Slices	View	No. of Slices
Meningioma	708	Transverse	154
		Sagittal	119
		Coronal	435
Glioma	1426	Transverse	604
		Sagittal	491
		Coronal	331
Pituitary	930	Transverse	236
		Sagittal	416
		Coronal	278
Healthy Control	501	Transverse	357
		Sagittal	97
		Coronal	47

B. *Brain Tumor Classification*

For Detection of Tumor Type and its corresponding ICD Code, we have developed a classification model, for which the proposed methodology is given below in Figure 3.

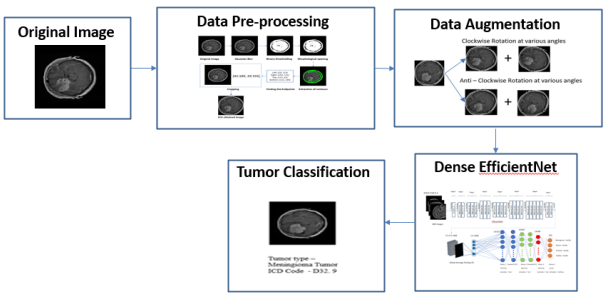

Fig. 3. MRI image of the brain tumors.

1) Data Pre Processing: The proposed method consists of extraction of the required image and mask according to their labels and a series of image processing methods to crop out the excess background whilst keeping only the part required ie. To extract the Region of Interest (ROI). This is done to improve the efficiency of training. First, the extracted image is converted to greyscale. Then, the Image is blurred a bit using Gaussian Blur to reduce image noise. Afterward, Binary threshold is applied to get a binary image based on setting a threshold value on the pixel intensity of the original image. The pixel intensity here is set from 45 to 255. Next, we find the shapes required for our model training using find contour and the contours are grabbed. Finally, we extract the contour position from left, right, top and bottom, and using the extracted contours, a new image is generated in which the excessive background is removed and only the part which is needed to detect tumor is kept.

2) Data Augmentation: The deep neural network needs large datasets for better results, but the dataset is limited. The dataset contains 3565 brain images, further divided into 80% for training, and 20% which remains for testing and validation purposes. The dataset is also heavily misbalanced between each class which can impact the training accuracy. So, data augmentation is needed to change in the minor. We have applied rotation for each class separately for the data requirement. We have rotated every single image in glioma tumor one time by 5 degrees counter clockwise, pituitary tumor two times by 5 degrees clockwise and counter clockwise and meningioma tumor three times by 5 degrees clockwise, counter clockwise also with 6 degrees counter clockwise and augmented them with the original image. This will enhance the amount of training data, allowing the model to learn more effectively. This may assist in increasing the quantity of relevant data. It contributes to the reduction of overfitting and enhances generalization. Data augmentation

(DA) is the process of creating additional samples to supplement an existing dataset via transformation. By data warping or oversampling, this augmentation exaggerated the size of the training dataset.

3) Dense EfficientNet: Before seeing about dense efficientnet, let us know about what is efficientnet, its modules, sub – blocks and the architecture of efficientnet. first. Efficientnet is a convolutional neural network architecture and scaling method that uses a compound coefficient to scale all depth/width/resolution dimensions evenly. The efficientnet scaling method consistently increases network breadth, depth, and resolution with a set of pre-set scaling coefficients [17]. Efficientnet scales up models with the help of a simple but effective technique known as compound coefficient. Instead of scaling up width, depth, or resolution at random, compound scaling scales each dimension equally with a given set of scaling coefficients [17]. To design the compound scaling method, the authors evaluated the effects of each scaling methodology on the model's performance and efficiency. While scaling single dimensions improves model performance, they reasoned that balancing the scale in all three dimensions (width, depth, and image resolution) improves overall model performance the most [17]. Figure 4 shows the architecture of an EfficientNet model. Let us now look into our architecture of dense efficientnet. This paper presents a novel dense CNN model that combines pre-trained efficientnet with dense layers. The dense block concept is made up of convolution layers the same size as the efficientnet input feature maps. Dense block uses the output feature maps of the preceding convolution layers to generate more feature maps with fewer convolution kernels. The dense efficientnet network has two layers: dense and drop-out. A dense layer is the basic layer that feeds all of the previous layer's outputs to all of its neurons, with each neuron providing one output to the next layer. The drop-out layer is used during training to reduce capacity or thin the network and avoid overfitting. The model begins by addition of a pooling layer followed by three dense layers and two drop-out layers to ensure the model runs smoothly. The numbers of neurons in the dense units are 720, 360, and 180, respectively. The drop-out values are 0.25, and 0.25 respectively. Finally, we have used a dense layer composed of four fully connected neurons in conjunction with a Softmax output layer to compute and classify the probability score for each class. Figure 5 illustrates the structure of the proposed efficientnet in detail.

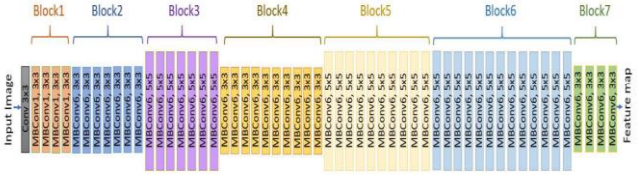

Fig. 4. EfficientNet CNN Model Architecture [18]

4) Hyperparameters set and Output Generated: Table II shows the hyperparameters set for our dense efficientnet b2 to get the accuracy. The outputs generated are tumor type and the corressponding ICD code for that tumor type which will be visible on the report.

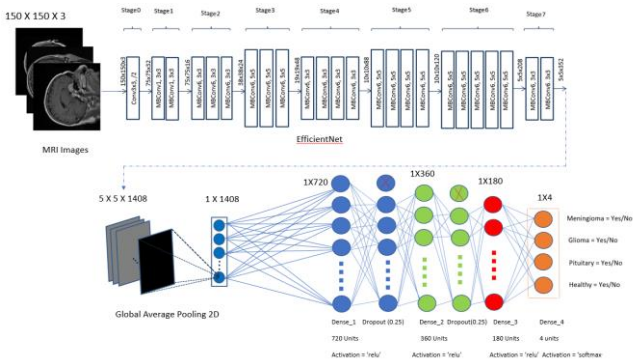

Fig. 5. Proposed Dense EfficientNet CNN Model Architecture

TABLE II. HYPERPARAMETERS FOR DENSE EFFICIENTNET

Hyperparameters	Values
Batch size	32
Epoch	20
Initial learning rate	0.0001
Reducing LOR at patience	2
Reducing LOR at factor	0.3
Optimizer	Adam

C. Brain Tumor Segmentation

For obtaining tumor radiomic characteristics, which is nothing but the tumor diameter and area, along with the original image with tumor region highlighted, we have developed a segmentation model, for which the proposed methodology is given below in Figure 6.

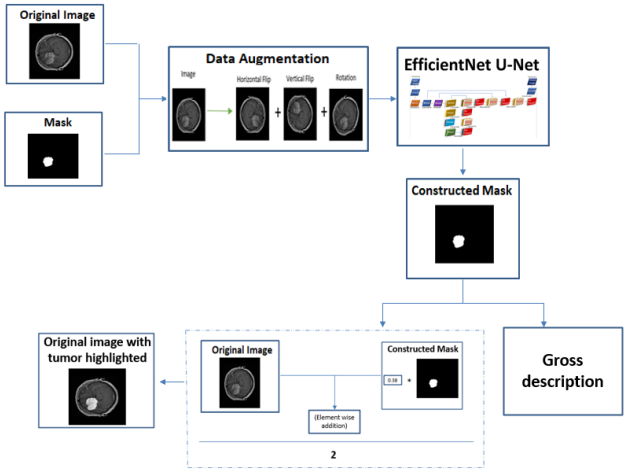

Fig. 6. Overview of proposed methodology for Brain Tumor Segmentation

1) Data Augumentation: To diversify the training data, the basic forms of data augmentation are used. The torchvision module of Pytorch is used for all augmentation methods. They are as follows: horizontally flip, vertically

flip, and rotate between 75 and -15 degrees. Each augmentation method has a probability of 0.5, and the order in which they are applied is also random. The degree of rotation for rotation augmentation is chosen at random between 75 and -15 degrees. Data augmentation for brain tumor segmentation is shown in Figure 3.12. The dataset is split in the ratio 80:20, where 80% is used for training the model and 10% is used for validation and 10% is used for testing. A total of 18384 images (9192 images and mask respectively) were obtained which will be utilized for the brain tumor segmentation.

2) EfficientNet UNet: Mingxing Tan et al. [19] introduced EfficientNet UNet, which is a neural network architecture that combines the well-known UNet and EfficientNet architectures. UNet architecture is widely used for image segmentation tasks, in which each pixel in an image is classified into different classes. The architecture is made up of an encoder and a decoder, with the encoder extracting high-level features from the input image and the decoder generating a segmentation map by upsampling the features to the original image size. The EfficientNet architecture, on the other hand, is intended to be memory and computation efficient while achieving state-of-the-art performance on image classification tasks. To balance the network's depth, width, and resolution, the architecture employs a compound scaling method. The strengths of both architectures are combined in the EfficientNet UNet architecture. It employs the EfficientNet as an encoder for efficient feature extraction and the UNet as a decoder for accurate segmentation. The architecture also includes skip connections between the encoder and decoder, which aid in the preservation of low-level features and the accuracy of segmentation. Figure 7 shows the architecture for EfficientNet UNet.

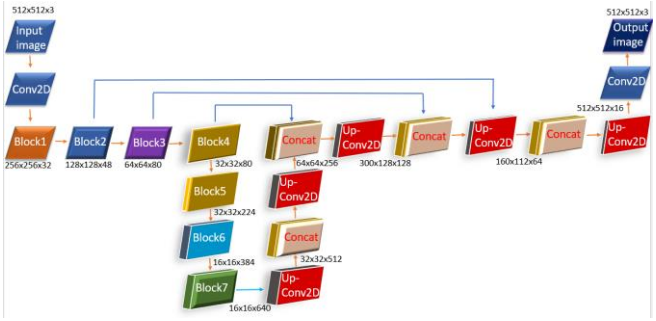

Fig. 7. EfficientNet UNet Architecture

3) Hyperparameters set and outputs generated: Table III shows the hyperparameters set for our U – net to get the maximum accuracy. A mask of the tumor will be generated using our U – net which will be utilized to find the outputs required for the tumor radiomic characteristics which are all given below.

TABLE III. HYPERPARAMETERS FOR EFFICIENTNET UNET

Hyperparameters	Values
Batch size	2
Epoch	20
Filters	[8, 16, 32, 64, 128]
Initial learning rate	0.001
Reducing LOR at patience	2
Reducing LOR at factor	0.85
Optimizer	Adam

D. Tumor Radiomic Characteristics

Radiomics is a quantitative approach to medical imaging, which provides a non-invasive approach to reliably extract quantitative features from radiographic images. The resulting features can be used to inform imaging diagnosis, prognosis, and therapy response [20].

The above EfficientNet UNet model is used by us for training our dataset and hence constructing a mask using the model for the images which we give as input as shown in Figure 8.

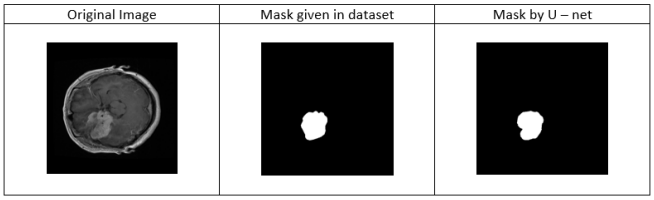

Fig. 8. Original image, mask given in the dataset and the mask built by EfficientNet UNet.

Using the above mask generated from our U – net, we can obtain the following outputs required to generate a preliminary diagnostic report of the brain tumor as shown in Figure 9.

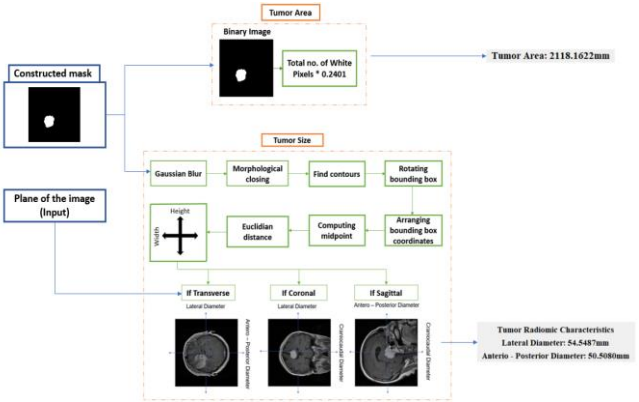

Fig. 9. Overview of the proposed methodology for obtaining the Tumor Radiomic Characteristics

For better visualization of the tumor, we can highlight the tumor in the original image by multiplying the mask generated by our U – net with a certain transparency range. The transparency level varies between 0 to 1 with 0 being completely transparent and 1 being completely opaque. We fixed the transparency range at 0.38 as this is optimal for visualization of the tumor. The multiplied mask generated by our U – net output is then added with the original image arguments elementwise and then divided by 2 to obtain the final output. Tumor diameter is defined as the maximal size of the invasive component of the primary tumor on pathologic examination. Tumor diameter is found by finding the contours in the mask generated by our U – net using the

contours we find the bounding box, and then unpack the ordered bounding box, then compute the midpoint between the top-left and top-right coordinates, followed by the midpoint between bottom-left and bottom-right coordinates. Using these midpoints, we find the Euclidian distance between these points. These points are multiplied with 0.49, where the pixel value is 0.49mm [11], thus getting the tumor diameter.

We can obtain three different diameters of the tumor using only two different oriented images. The three different diameters are:

- **Craniocaudal Diameter (d_{cc})** – along the long axis of the endometrial cavity
- **Antero – Posterior Diameter (d_{ap})** – along the anterior and posterior side of our brain
- **Lateral Diameter (d_l)** – along the lateral side of our brain

We can obtain craniocaudal diameter from either sagittal or coronal plane, antero – posterior diameter from either transverse or sagittal plane and lateral diameter from either transverse or coronal plane. By giving the image and the orientation of the image as input, we can obtain the diameters of the tumor as shown below in figure 10. Tumor area is calculated by converting the mask generated by our U – net into a binary image, taking the total count of the white pixels in the region, and multiplying it by 0.49 * 0.49 mm.

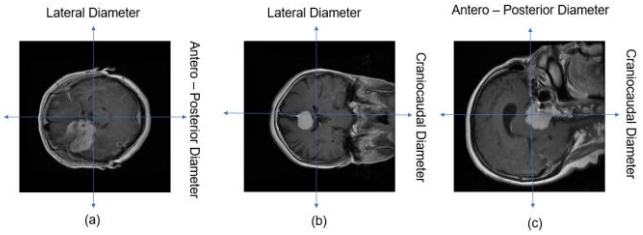

Fig. 10. (a) Transverse Plane and it's Diameter, (b) Coronal Plane and it's Diameter, (c) Sagittal Plane and it's Diameter

The outputs generated are tumor diameter along with the tumor area which are all the tumor radiomic characteristics, which will be printed in the preliminary report.

E. Preliminary Report Generation

A preliminary report will be generated automatically, in which it takes the following input.

- Input Image (T1 – Weighted Contrast Enhanced MRI Images)
- Plane of the Input Image (Transverse or Sagittal or Coronal)

The following outputs will be generated in the preliminary report.

- Original image with tumor highlighted
- Tumor type and its ICD code
- Tumor diameter
- Tumor area

Figure 11 shows the algorithm behind the preliminary report generation. First, we get input from user which is then fed into our classification algorithm, using that we get the tumor type. If the tumor type is none (i.e.) Healthy, then the whole segmentation algorithm process is skipped, and the tumor radiomic characterisitics will be displayed as "NA" in the output, else then the segmentation and tumor radiomics algorithm process will be gone through from which we will get the tumor radiomic characterisitcs (i.e.) tumor diameter and area in our preliminary report.

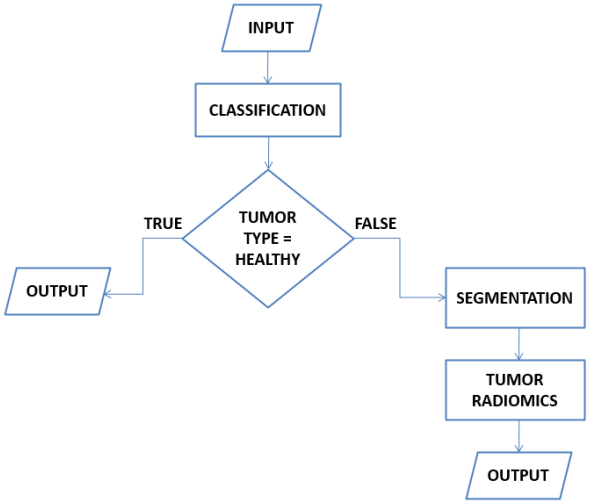

Fig. 11. Algorithm for Preliminary report generation

The Input text box and button GUI is designed using Python Tkinter for user convinience. The standard Python interface to the Tcl/Tk GUI toolkit is the tkinter package ("Tk interface"). Tk and tkinter are both available on most Unix platforms, including macOS, as well as Windows. [21]. One primary widgets were used here for our paper in Tkinter and one from PIL module. They are: tkinter.label and PIL.Imagetk respectively. tkinter.label is a widget that is used to implement display boxes where you can place text or images. The ImageTk module contains support to create and modify Tkinter BitmapImage and PhotoImage objects from PIL images. Figure 12 shows the entire preliminary report.

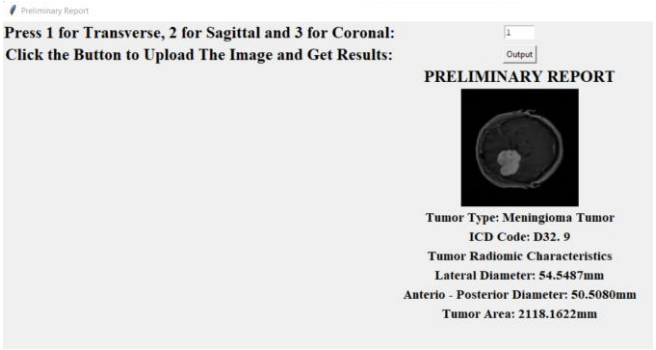

Fig. 12. Preliminary Report

IV. Results and Discussion

Several experimental tests have been performed to determine the validity of the proposed dense CNN model. All of the experiments were carried out in a Python programming environment with GPU support. Pre-processing is performed first, in which the images are cropped for better training and then augmented for training.

A. Evaluation Metrics

1) Accuracy: Accuracy is defined as the ratio of correct predictions to total samples.

2) Loss Function: A loss function is a mathematical function that measures how well a model can predict based on the input data. The goal of model training is to minimize the value of the loss function. The loss function compares the model's predicted outputs to the true outputs of the training data and computes a measure of the difference between them.

3) True Positive (Tp): A test result that correctly indicates the presence of a condition or characteristic [22].

4) False Positive (Fp): A test result which wrongly indicates that particular condition or attribute is present [22].

5) True Negative (Tn): A test result that correctly indicates the absence of a condition or characteristic [22].

6) False Negative (Fn): A test result which wrongly indicates that a particular condition or attribute is absent [22].

7) Precision: The precision is determined by dividing the number of correctly classified Positive samples by the total number of Positive samples (either correctly or incorrectly). The precision of the model indicates how accurate it is at classifying Positive samples. [22].

$$Precision = \frac{Tp}{Tp + Fp} \quad (1)$$

8) Recall: The recall is calculated by dividing the total number of Positive samples by the percentage of Positive samples correctly classified as Positive. The recall measures the model's ability to recognise Positive samples. The greater the recall, the more positive samples discovered. [22].

$$Recall = \frac{Tp}{Tp + Fn} \quad (2)$$

9) F1 Score: The F1-score is a model accuracy metric that determines how accurate a model is on a given dataset. It is the harmonic mean of the model's precision and recall, and it is a method of combining the model's accuracy and recall [22]. A perfect model has an F-score of 1.

$$F1\ score = \frac{2}{\frac{1}{Recall} * \frac{1}{Precision}} \quad (3)$$

10) Sorensen – Dice Coefficient: The Dice score is often used to quantify the performance of image segmentation methods. There, annotation of some ground truth region in the image is done and then an automated algorithm is made to do it. The validation of the algorithm is done by calculating the Dice score, which is a measure of how similar the objects are. So, it is the size of the overlap of the two segmentations divided by the total size of the two objects. Using the same terms as describing accuracy, the Dice score is [23]:

$$Dice\ Score = \frac{2 * Tp}{2 * Tp + Fp + Fn} \quad (4)$$

11) Jaccard Similarity Index: The Jaccard similarity index (also known as Intersection over Union (IoU)) compares members from two sets to determine which are shared and which are distinct. It is a measure of similarity between two sets of data, with a scale ranging from 0% to 100%. The higher the percentage, the closer the two populations are [24].

$$J(A,B) = \frac{|A \cap B|}{|A \cup B|} \quad (5)$$

Where, J = Jaccard Similarity Index or Intersection over Union, A = Ground Truth Image, B = Predicted Image.

B. Brain Tumor Classification

Table IV shows the training and validation accuracy for dense efficientnet b0 to b7 value.

TABLE IV. DENSE EFFICIENTNET MODELS AND THEIR ACCURACIES

Dense EfficientNet Models	Training Accuracy	Validation Accuracy
Dense EfficientNet B0	99.81%	97.34%
Dense EfficientNet B1	99.89%	98.15%
Dense EfficientNet B2	99.93%	97.63%
Dense EfficientNet B3	99.91%	97.58%
Dense EfficientNet B4	99.90%	97.10%
Dense EfficientNet B5	99.84%	97.34%
Dense EfficientNet B6	99.85%	97.57%
Dense EfficientNet B7	99.84%	97.46%

It is seen from above table that efficientnet b2 has the highest training and validation accuracy. Hence, we are considering efficientnet b2 for our dense efficientnet classification model and is further evaluated using loss, accuracy, precision, recall and f1 score.

1) Loss and Accuracy: To improve accuracy, the proposed model activated the augmented tumors. The loss function here is "categorical crossentropy". The proposed model showed 99.93% accuracy on training data and 97.63% accuracy on the testing dataset which is plotted in Figure 13.

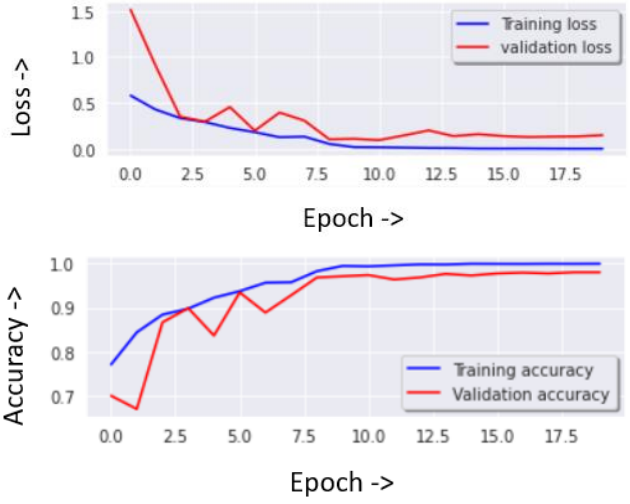

Fig. 13. Loss and Accuracy of Dense EfficientNet B2.

The experiment has been performed in 20 epochs. A batch size of 32, image size 150 x 150, and verbose 1 have been considered for the experiment. In the accuracy model shown in above figure 13, initial validation accuracy is around 0.7013 but after two epochs the validation accuracy suddenly increases to nearly 0.8670. In the same manner, as seen in figure 13, the initial validation loss is 1.1516 but after two epochs the loss decreases to 0.3502. As shown in Figure 13 and 4.2, there is a positive trend toward improving accuracy and reducing loss. At first, validation accuracy is low, but it progressively improves to almost 97 percent. The testing accuracy and testing loss of Dense EfficientNetB2 is 97.63% and 0.1493 respectively.

2) Confusion Matrix: To compare the performance of the proposed model, various performance measures such as accuracy, precision, recall, and F1-score were used. The confusion matrix was used to evaluate these parameters. The details were also examined using the confusion matrix which is shown below in Figure 14. For comparison of different techniques, three important measures have been considered: precision, recall, and F1-score.

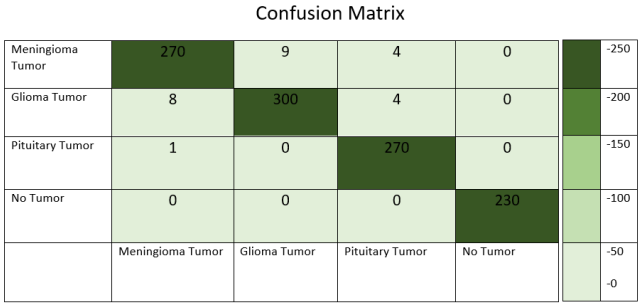

Fig. 14. Confusion Matrix for Dense EfficientNet B2

The confusion matrix presents misclassifications because of overfitting using 10% of testing data obtained from the original dataset. From the matrix it is observed that the misclassified tumors in the proposed Dense EfficientNet B2 is 9 out of 1096 testing images. Due to lesser amounts of misclassified data, the accuracy of the proposed model is higher than the others. Most of the misclassified samples belong to the ”meningioma” class which cannot learn as effectively as the other three.

3) Classification Report: For comparison of different techniques, three important measures have been considered: precision, recall, and F1-score. Figure 15 shows the classification report of the dense efficientnet b2. It is observed from Table IV that Dense EfficientNetB2 has the highest precision, recall, and F1-score when compared with other models. The no tumor has the best performance in all measurements when compared to other types of tumors. All the values of precision, recall, and F1-score of pituitary tumors are quite good. The overall results of the dense EfficientNetB2 are excellent. The accuracy, precision, and F1-score of the proposed method are 97.63%, 98%, and 98%, respectively, which is better than other comparison methods. Based on Table IV, dense EfficientNet B2 outperforms other techniques because deep-learning-based approaches are more efficient and capable of handling large amounts of data for classification.

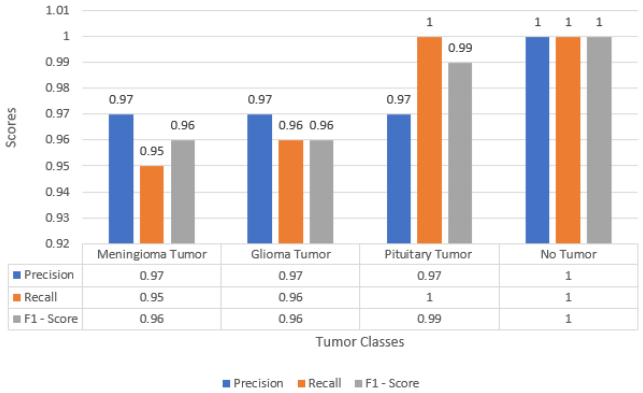

Fig. 15. Classification Report for Dense EfficientNet B2

4) Discussion: Table V shows the accuracy of our model at each plane and the class of the tumor.

TABLE V. ACCURACY OF EACH PLANES AND TUMOR CLASS

Image Plane	Accuracy	Tumor Class	Accuracy
Transverse	98.84%	Meningioma	96%
		Glioma	98%
		Pituitary	99%
		Healthy	100%
Sagittal	99.29%	Meningioma	98%
		Glioma	99%
		Pituitary	100%
		Healthy	100%
Coronal	99.42%	Meningioma	99%
		Glioma	99%
		Pituitary	99%
		Healthy	100%

We can see from the table that our model performs best in coronal plane whereas it performs comparatively less in transversal plane. This might be due to misbalancing of the data between classes being comparatively higher in transversal plane than in coronal plane. We can also see that healthy control images performs the best when comparing to other classes. This is due to the healthy control image having no tumor inside them which makes them easy to distinguish. Meningioma and Glioma class has lower percentage when comparing to pituitary and healthy control. Among the three types of tumor classes, Pituitary performs the best and meningioma performs comparatively less. This is due to meningioma class having less data when comparing to pituitary class.

C. Brain Tumor Segmentation

The training is run on google colab with the single 12GB NVIDIA Tesla K80 GPU [26] that can be used up to 12 hours continuously. Total time taken for model training was 1 hours and 30 minutes. We started with an initial learning rate of 1e-4 and reduced it by 85% on plateauing, final learning rate at the end of 20 epochs was 1.25e-5.

Table VI shows the training and validation IoU for efficientnet unet b0 to b7 value.

TABLE VI. EFFICIENTNET UNET MODELS AND THEIR IOU

Dense EfficientNet Models	Training IoU	Validation IoU
Dense EfficientNet B0	0.765401	0.566200
Dense EfficientNet B1	0.535473	0.493138
Dense EfficientNet B2	0.559616	0.509402
Dense EfficientNet B3	0.715273	0.573642
Dense EfficientNet B4	0.622266	0.536767
Dense EfficientNet B5	0.692441	0.571719
Dense EfficientNet B6	0.598968	0.531488
Dense EfficientNet B7	0.632277	0.540451

It is seen from above table that efficientnet b3 has the highest training and validation accuracy. Hence, we are considering efficientnet b3 for our dense efficientnet classification model and is further evaluated using loss, Dice score, and Jaccard Similarity Index (IoU).

1) Loss Function: The loss function here is "Dice Loss". The graph indicating Loss Value over 20 epochs are given below in Figure 16.

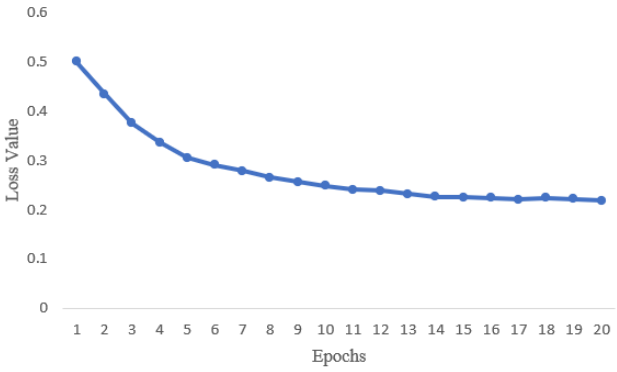

Fig. 16. Loss plot for EfficientNet UNet B3

2) Discussion: Table VII shows a summary of the various performance metrics of our EfficientNet UNet model. Two different metrics were used for evaluation of our model. They are Sorensen Dice Coefficient, and Jaccard Similarity Index. However, the main performance metrics which is most commonly used for evaluation of segmentation models is Jaccard Similarity Index, also known as Intersection over Union (IoU). Our model has gained a IoU of 0.715273. There is room for improving the model accuracy which can be achieved by changes in hyperparameters etc. But for this EfficientNet UNet, the hyperparameters set was optimal to our computational specification as we are limited by our computational capability.

TABLE VII. EFFICIENTNET UNET PERFORMANCE METRICS

EfficientNet UNet [8, 16, 32, 64, 128]		
Evaluation Metrics	***Training***	***Validation***
Sorensen Dice Coefficient	0.786656	0.700826
Jaccard Similarity Index	0.715273	0.573642

V. CONCLUSION

In this paper, we present an EfficientNet based detection and diagnosis of brain tumor using MRI Images, where we build a system which automatically generates a preliminary report which contains the type of tumor, ICD code, tumor diameter and tumor area along with the original input image with the tumor highlighted for visualization.

The major limitation of this paper is in the accuracy of segmentation, which is only around 71%. Another limitation lies in the fact that, the dataset which we had utilized lacks demographics details of the patient. This had limited our scope of the paper to just diagnosing tumor diameter and area. Obtaining patient demographic details opens more scope for improvement in diagnosis of brain tumor, especially in finding of tumor volume and tumor growth rate.

Some scope for improvement can be done in adding more classes of brain tumor so that we can detect and diagnose more brain tumor diseases. This work only utilizes .png images which are not the medical standard for detection and diagnosis. Using .dicom images will be the medical standard.

Nowadays, the issue of automated detection and diagnosis of brain tumors are major research area. Our work, which is automating the process of detection, diagnosis, and generation of a preliminary diagnosis report of the brain tumor will aid the radiologist and physician and will aid in more research work in the automation of the detection and diagnosis of brain tumor.

REFERENCES

[1] "Brain Cancer Symptoms, Causes and Treatment in India - Apollo Hospitals", Apollo Hospitals, 2022. [Online]. Available: https://www.apollohospitals.com/departments/cancer/organ-cancer/brain-central-nervous-system/.

[2] "Brain Tumor - Statistics", Cancer.Net, 2022. [Online]. Available: https://www.cancer.net/cancer-types/brain-tumor/statistics.

[3] "Meningioma - Symptoms and causes", Mayo Clinic, 2022. [Online]. Available:https://www.mayoclinic.org/diseasesconditions/meningioma/symptoms-causes/syc-20355643.

[4] "Glioma - Symptoms and causes", Mayo Clinic, 2022. [Online]. Available:https://www.mayoclinic.org/diseases/conditions/glioma/symptoms-causes/syc-20350251.

[5] "Pituitary tumors - Symptoms and causes", Mayo Clinic, 2022. [Online]. Available: https://www.mayoclinic.org/diseases-conditions/pituitary-tumors/symptoms-causes/syc-20350548.

[6] "Brain Tumor - Diagnosis", Cancer.Net, 2022. [Online]. Available: https://www.cancer.net/cancer-types/brain-tumor/diagnosis.

[7] "International Classification of Diseases (ICD)", *Who.int*, 2022. Available:https://www.who.int/standards/classifications/classification-of-diseases.

[8] A. Chen, J. Ryu, P. Donald, and A. Colevas, "Cancer of the Nasal Cavity and Paranasal Sinuses", 2022.

[9] S. M. Shelke and S. W. Mohod, "Automated Segmentation and Detection of Brain Tumor from MRI", Ieeexplore.ieee.org, 2022. [Online]. Available: https://ieeexplore.ieee.org/document/8554807/.

[10] M. Huang et al., "Content-Based Image Retrieval Using Spatial Layout Information in Brain Tumor T1-Weighted Contrast-Enhanced MR Images", PLoS ONE, vol. 9, no. 7, p. e102754, 2014. Available: 10.1371/journal.pone.0102754.

[11] J. Cheng et al., "Correction: Enhanced Performance of Brain Tumor Classification via Tumor Region Augmentation and Partition", PLOS ONE, vol. 10, no. 12, p. e0144479, 2015. Available: 10.1371/journal.pone.0144479.

[12] H. H. Sultan, N. M. Salem, and W. Al-Atabany, "Multi-Classification of Brain Tumor Images Using Deep Neural Network," in IEEE Access, vol. 7, pp. 69215-69225, 2019, doi: 10.1109/ACCESS.2019.2919122.

[13] A. Alqudah, "Brain Tumor Classification Using Deep Learning Technique - A Comparison between Cropped, Uncropped, and

Segmented Lesion Images with Different Sizes", International Journal of Advanced Trends in Computer Science and Engineering, vol. 8, no. 6, pp. 3684-3691, 2019. Available: 10.30534/ijatcse/2019/155862019.

[14] E. Irmak, "Multi-Classification of Brain Tumor MRI Images Using Deep Convolutional Neural Network with Fully Optimized Framework", Iranian Journal of Science and Technology, Transactions of Electrical Engineering, vol. 45, no. 3, pp. 1015-1036, 2021. Available: 10.1007/s40998-021-00426-9

[15] "brain tumor dataset", figshare, 2022. [Online]. Available: https://figshare.com/articles/dataset/brain_tumor_dataset/1512427.

[16] “Brain Tumor MRI Dataset" , Kaggle.com, 2022. [Online]. Available: https://www.kaggle.com/datasets/masoudnickparvar/brain-tumor-mri-dataset.

[17] “Complete Architectural Details of all EfficientNet Models”, Medium, 2022. [Online]. Available: https://towardsdatascience.com/complete-architectural-details-of-all-efficientnet-models-5fd5b736142.

[18] Baheti, B. et al. (2020) “EFF-UNet: A novel architecture for semantic segmentation in unstructured environment,” 2020 IEEE/CVF Conference on Computer Vision and Pattern Recognition Workshops (CVPRW) [Preprint]. Available at: https://doi.org/10.1109/cvprw50498.2020.00187.

[19] M. Tan and Q. V. Le, "EfficientNet-UNet: A Fast and Scalable Model for Medical Image Segmentation," in International Conference on Medical Image Computing and Computer-Assisted Intervention, 2020, pp. 405-415.

[20] M. Zhou et al., "Radiomics in Brain Tumor: Image Assessment, Quantitative Feature Descriptors, and Machine-Learning Approaches", American Journal of Neuroradiology, vol. 39, no. 2, pp. 208-216, 2017. doi: 10.3174/ajnr.a5391.

[21] "tkinter — Python interface to Tcl/Tk — Python 3.10.4 documentation", Docs.python.org, 2022. [Online]. Available: https://docs.python.org/3/library/tkinter.html

[22] "mAP (mean Average Precision) might confuse you!", Medium, 2022. [Online]. Available: https://towardsdatascience.com/map-mean-average-precision-might-confuse-you-5956f1bfa9e2.

[23] "Is the Dice coefficient the same as accuracy?", Cross Validated, 2022. Available: https://stats.stackexchange.com/questions/195006/

[24] "Jaccard Index / Similarity Coefficient", Statistics How To, 2022. Available: https://www.statisticshowto.com/jaccardindex/

[25] “Google Colab", Research.google.com, 2022. https://research.google.com/colaboratory/faq.html.